Phys Chem Minerals (1999) 26: 484–495

ORIGINAL PAPER

M. Gambhir · M.T. Dove · V. Heine

Rigid unit modes and dynamic disorder: SiO_2 cristobalite and quartz

Received: 10 March 1998 / Revised, accepted 15 January 1999

Abstract The high temperature (β) phases of SiO_2 cristobalite and quartz are studied by performing molecular dynamics simulations using a model which allows easy analysis of tetrahedral motions. The dynamic nature of the disordered high-temperature phase of cristobalite is attributed to rigid unit mode (RUM) excitations, and it is found that the entire spectrum of RUMs is responsible for the disorder. Comparisons of the results of β-cristobalite with those of β-quartz lead to the conclusion that framework structures with high degrees of geometric flexibility, and hence many RUMs, are free to deform through cooperative tetrahedral rotations even in the limit of extremely large tetrahedral stiffnesses.

1 Introduction

Many framework mineral structures consist of stiff polyhedral units, made up of two or more atoms, such as SiO_4 tetrahedra. These stiff units are loosely jointed with one another and the characteristic inter-polyhedral force constant (stiffness) is often 25–100 times smaller than the intra-polyhedral stiffness. It has been found that there exist a few motions of the system which only involve coherent rotations and/or translations of the polyhedra with zero distortion of the stiff units. These motions are, therefore, of very low energies. They are called rigid unit modes (RUMs) and are determined geometrically by moving the constituent units without distortion (Dove et al. 1993, 1995; Dove 1997b; Hammonds et al. 1994). It should be stressed that the units are deformable and practically all phonon modes involve their deformation, but there are also motions that may be accomplished without deformation which are especially important because of the stiffness of the polyhedra. In the structure of Fig. 1, showing the view down a ⟨111⟩ direction in the high-temperature β-phase of cristobalite, such motions occur when adjacent tetrahedra rotate in opposite directions through the same angle.

The exploration of the RUM model has illuminated several phenomena, particularly the reasons for the widespread occurrence of displacive phase transitions in framework structures (Hammonds et al. 1996), the phase transition temperatures (Dove et al. 1995), negative coefficients of thermal expansion (Pryde et al. 1996, 1998; Welche et al. 1998), possible adsorption sites for catalyst ions in zeolites (Hammonds et al. 1997, 1998), the origins of thermal diffuse X-ray and electron scattering patterns (Hammonds et al. 1996; Dove et al. 1996b) and, recently, a possible explanation of the low frequency dynamics in silica glasses (Dove et al. 1997b; Trachenko et al. 1998).

It has been found that the number of geometrically allowed RUMs varies greatly from structure to structure (Hammonds et al. 1996). Even among the family of tetrahedral framework structures in which all corners of all tetrahedra are linked to other tetrahedra, there are great variations. For example, zeolites such as faujasite have very many RUMs (Hammonds et al., 1997, 1998), whereas the low-temperature α-phase of cristobalite has very few (Hammonds et al., 1996).

The aim of the present work is to use this model to provide an understanding of the atomic structure of the high-temperature β-phase of SiO_2 cristobalite. Cristobalite undergoes a displacive phase transition from the high-symmetry β-phase to the lower-symmetry α-phase on cooling below 548 K. The α-phase is well understood and the RUM instability at the X-point of the Brillouin zone which is responsible for the rotations and translations from the $\beta \longrightarrow \alpha$ forms has been identified and documented (Swainson and Dove 1993a, b; Hammonds et al. 1996).

M. Gambhir · M.T. Dove (✉)
Department of Earth Sciences, University of Cambridge, Downing Street, Cambridge CB2 3EQ, United Kingdom

V. Heine
Cavendish Laboratory, University of Cambridge, Madingley Road, Cambridge CB3 0HE, United Kingdom

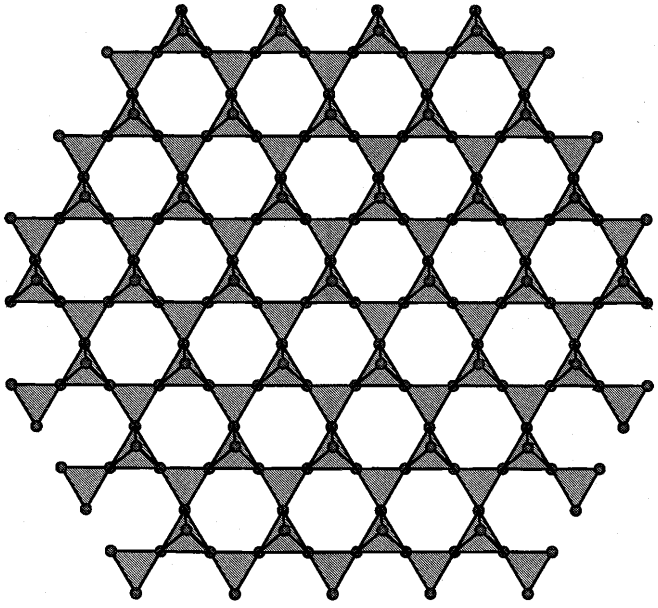

Fig. 1 Plan view of a (111) layer in ideal β-cristobalite

The problem with β-cristobalite that will be addressed here is that it would seem to be a dynamically disordered structure. X-ray (Wright and Leadbetter 1975) and neutron (Schmahl et al. 1992) diffraction experiments show that the system has an overall $Fd\bar{3}m$ symmetry and this suggests that, in a static completely ordered model, the Si—O—Si angles are 180° as in Fig. 1. Diffraction results, however, give an idealised structure, averaged over space and time, so locally the symmetry may deviate from the overall space group. The lattice parameter of the cubic unit cell is 7.15 Å and the silicon-oxygen distance is 1.61 Å with the tetrahedra almost completely undeformed (Wright and Leadbetter 1975; Schmahl et al., 1992; Swainson and Dove 1995a, b). Therefore, given that the tetrahedra are very stiff, the lattice parameter is too small to allow a fully expanded, *idealised*, cristobalite structure to be responsible for the diffraction results. The 180° Si—O—Si angle is uncommon and is generally found to be around 140°–150° in other silicates.

It has been concluded, therefore, that the tetrahedra are tilted away from the directions prescribed by the idealised structure and that the Si—O—Si angles do lie between the common values. The lattice parameter and Si—O distance measured imply, for undeformed tetrahedra, Si—O—Si angles of approximately 148°. Recent neutron total scattering measurements on β-cristobalite (Dove et al. 1997a) have shown that, indeed, almost completely undistorted tetrahedra are tilted away from their ideal orientations to give an average angle between the actual Si—O bond vector and the ⟨111⟩ axes of around 17°. However, because the overall symmetry of the system must remain cubic $Fd\bar{3}m$ the rotations (and accompanying translation) of the tetrahedra must be disordered. This will be referred to as the *real* structure. Incidentally, it is seen that rotations must be accompanied by translations in order to keep the tetrahedra minimally deformed.

The purpose of this work is to use a molecular dynamics simulation (MDS) to elucidate the nature of the orientational disorder in greater detail. The β-cristobalite structure has whole planes of RUMs in wave vector space and the great many modes of low energy distortion available to it may permit a dynamically disordered state to exist (Swainson and Dove 1993a, 1995b). Dynamic disorder is characterised by extremely short-ranged correlations, in time and space, of orientations of tetrahedra. However, a dynamic state is not the only possibility and previous studies have suggested that the β-phase consists of patches of a lower symmetry crystalline state brought about through coherent rotations and translations which locally resemble the α phase. These patches have been predicted to have an appreciable (several unit cells) extent in space and time (several low frequency phonon periods). There have been two major proposals for the statically disordered structure. The first (Wright and Leadbetter 1975; Liu et al. 1993a; Demkov et al. 1995) states that the local symmetry of the structure is $I\bar{4}2d$, and the RUM responsible will have zero wave vector (Swainson and Dove 1993b), and the second (Hatch and Ghose 1991) has the local symmetry of the α phase ($P4_12_12$) and therefore the RUMs responsible lie at the X points. Both models propose the existence of a patchwork of microdomains resulting in the oxygen atoms lying on annuli around the ⟨111⟩ axes in six partially occupied positions. By contrast, the total neutron scattering results for β-cristobalite of Dove et al. (1997a) appear to rule out the latter domain model.

The nature of the structure of the β-phase over short length scales is unknown, and this study attempts to answer the question of whether the disorder is dynamic or static. This is achieved through the analysis of spatial and temporal correlations in the structure generated in the computer simulations.

The MDS of this study is concerned with the *real* cristobalite structure but it will be convenient to refer back to the simple, idealised structure to aid interpretation. The real structure can be seen as a coordinated set of finite rotations of the tetrahedra from the notional idealised structure. As explained, the motions of interest are the RUMs because these have the lowest associated energy and so we expect them, and those motions close to RUMs, to be of the largest amplitude and hence to dominate. It should be noted that distortions of the tetrahedra at high temperatures are slight due to their stiffness (Downs et al. 1992) so the distortions in this simulation are very small and hence motions may be approximated to RUMs. So, we will be interested in the infinitesimal RUM phonons of the idealised structure, bearing in mind that they are excited to quite large finite amplitudes. RUMs with infinitesimal amplitudes may be superposed upon one another as for simple phonon modes of the structure. However, since RUMs involve rotations of the tetrahedra, they

may not be so easily superposed at finite amplitudes due to the non-commutivity of rotations (Hammonds et al. 1996). The possibility exists that the excitation of some RUMs may preclude the existence of others. Indeed, it has been proposed (Liu et al. 1993b; see the reply by Swainson and Dove 1993b) that, at temperatures for which tetrahedral rotations are large, selections of certain RUMs may exist, with others being excluded, and the formation of microdomains *could* be the result of this process. The MDS therefore also seeks to answer the question of whether a framework system's entire set of RUMs can be excited simultaneously to give a large number of low energy distortions contributing to a dynamic disorder.

2 The molecular dynamics model

Our MDS was performed using a simplified model wherein rigid ideal SiO_4 tetrahedra interacted with neighbouring tetrahedra through harmonic forces acting on the linked corners, giving zero equilibrium separation. This is the dynamic version of the "split-atom" method proposed by Giddy et al. (1993). The force constant is formally equivalent to the stiffness of the tetrahedra, and in our model is the only parameter controlling the dynamic simulation other than the volume. Although this force constant gives harmonic motion for uniform displacements of the tetrahedra, it actually translates to anharmonic motions when the tetrahedra rotate if, as in our work, the dynamical equations of motion are expressed in terms of orientational variables. Anharmonicity in the equations of motion is essential for molecular dynamics simulations to work properly, with transfer of energy between different vibrational modes.

In addition to discovering the nature of β-cristobalite, it was also the aim of these simulations to illuminate issues pertaining to the degree of flexibility of structures that have RUMs. As already stated, different structures have very different degrees of RUM flexibility. By making the stiffness 10 times larger, as was possible in these simulations, we could effectively *freeze out* all motions except those of RUM type or very close to it. The effect of a severely reduced amount of non-RUM flexibility in the structure could be gauged by examining tetrahedral localisations (see Sect. 5). To this end, β-quartz was compared with β-cristobalite since the structures' RUM spectra are rather different – β-cristobalite having many more RUMs than β-quartz (Hammonds et al., 1996).

The model included the essential physical ingredients necessary for the analysis of these problems: the stiffness of the tetrahedra, which is the dominating force, was explicitly included; the volume of the system is governed by the interplay between the inward pressure due to attractive forces, which tend to collapse the structure to the α-phase, and the vibrational entropy which effectively exerts an outward pressure (but see the discussion of the thermal expansion by Swainson and Dove 1995a, and the follow-up measurements of Bourova and Richet 1998). In our model the volume was fixed at the experimental value for 1000 K. Reducing the number of system variables in this way allowed all results to be interpreted easily in terms of tetrahedral motions and RUMs.

The molecular dynamics algorithm used was of the type NVE, conserving the number of molecules, the volume of the system and the total energy. The algorithm was designed for use with molecules and other units and the results were easily interpretable in terms of translations and rotations of tetrahedra. Rotations were handled with the use of quaternions. Periodic boundary conditions were used, and the size and shape of the sample was *not* allowed to vary. A time step of 0.001 ps was found to be sufficiently small to prevent total energy drifts and allow the observation of even the highest frequency modes of oscillation (these were approximately 20 THz). The system was equilibrated for 10 000 time steps (10 ps) before the statistical quantities required were accumulated. Quantities which were thermally averaged, such as the example given later, were typically averaged over a time period of 100 000 time steps (100 ps).

The split-atom force constant was assigned a value that best reproduced the range of frequencies of quartz in a lattice dynamics calculation.

2.1 Cristobalite

The MDS system was a cubic box of dimensions $16a \times 16a \times 16a$ where a is the lattice parameter of β-cristobalite and each unit cube contained 8 tetrahedra.

The types of quantity calculated are generally expressible in the form of correlation functions. Probably the most important of these is the scattering factor, $S(\mathbf{k})$, which is defined following chapter 12 of Dove (1993). The degrees of freedom of the tetrahedra are labelled $u_i(\mathbf{R}, t)$ where i runs from 1–12 for each pair of tetrahedra covering the three translational and rotational degrees of freedom of each tetrahedron. The vector $\mathbf{R}$ represents the primitive cell position (two tetrahedra per cell) and t is the time. The collective variables are:

$$u_i(\mathbf{k}, t) = \sqrt{\frac{m_i}{N}} \sum_{\mathbf{R}} u_i(\mathbf{l}, t) \mathrm{e}^{i\mathbf{k}.\mathbf{l}} \quad , \tag{1}$$

where m_i is the mass or moment of inertia of a tetrahedron. The constant N is the number of pairs of tetrahedra in the sample and $\mathbf{k}$ is a permitted $\mathbf{k}$-point lying on the grid of points in $\mathbf{k}$ space as dictated by the periodic boundary conditions.

The matrix $S_{ij}(\mathbf{k})$ is produced by averaging products of these collective variables over the period of the simulation:

$$S_{ij}(\mathbf{k}) = \langle u_i(\mathbf{k}, t) u_j^*(\mathbf{k}, t) \rangle \quad , \tag{2}$$

where the angled brackets $\langle \cdots \rangle$ represent a thermal average.

When the matrix $S_{ij}(\mathbf{k})$ is diagonalised, the 12 normalised eigenvectors of the matrix give the phonon (=normal mode) translations and rotations, and the eigenvalues, Λ_n, are related to the amplitudes $Q_n(\mathbf{k})$ to which these normal modes are excited:

$$\Lambda_n = \langle Q_n(\mathbf{k}) Q_n^*(\mathbf{k}) \rangle \quad . \tag{3}$$

For a harmonic system at temperature T we also have:

$$\langle Q_n(\mathbf{k}) Q_n^*(\mathbf{k}) \rangle = \frac{k_\mathrm{B} T}{\omega_n^2(\mathbf{k})} \quad , \tag{4}$$

For our 'real' structure the situation is inherently different. At least the rotations $u_i(\mathbf{l}, t)$, and probably also the translations, are non-zero, not just because of thermal excitation, but because of the inherent nature of the dynamically disordered state, i.e. because of the inherently non-zero values of the rotations needed to fit the tetrahedra into the required volume. We expect the amplitude squared $\langle Q_n(\mathbf{k}) Q_n^*(\mathbf{k}) \rangle$ will still be given approximately by Eq. (4) for modes far from RUMs. However, for modes close to the RUMs inherent in the fluctuating disordered state, we expect their amplitudes to be largely determined by the finite rotations needed in that state rather than by thermal excitation. These expectations will be tested.

Two real space correlation functions were also calculated during the simulation runs. One of these, a spatial correlation function $f_{sp}(\mathbf{r})$, described the rotational correlation between one tetrahedron and all others lying in certain planes of the structure:

$$f_{sp}(\mathbf{r}) = \langle \phi(0) \phi(\mathbf{r}) \rangle \quad , \tag{5}$$

where $\phi(\mathbf{r})$ represents a rotational angle of a tetrahedron about a particular axis at the position vector $\mathbf{r}$ from the origin. In addition to this, time-dependent correlation functions were also calculated. The functions were computed as generally as possible by obtaining correlations of each degree of freedom (translations and rotations) with every other for a pair of tetrahedra. These functions were averaged out over the simulation time and over the entire sample of tetrahedral pairs.

$$g_{ij}(t) = \langle u_i(0)u_j(t)\rangle \quad (6)$$

here g_{ij} represents one of the 12×12 correlation matrix elements and the $u_i(t)$ represent the 12 degrees of freedom of a pair of tetrahedra as functions of time. Both spatial and temporal correlation functions were computed over an accumulation period of 100 000 time steps.

It should be noted that, thermodynamically, the model depends only on one parameter, s, which is a measure of the stiffness of the tetrahedra:

$$s = \frac{\lambda}{k_B T} \quad (7)$$

This ratio provides a comparison between the potential and kinetic energies of the system as found in the exponent of the thermodynamic Boltzmann factor. Increasing the parameter s by a factor of ten may be interpreted either as an increase, by a factor of ten, of the stiffness of the tetrahedra at constant temperature, or as a decrease of the temperature by the same factor at constant stiffness. In the former interpretation this stiffness value is *very* large (superstiff) and it allowed us to study the level of flexibility of the system when the polyhedral units were very inflexible, effectively freezing out all motions except the RUMs. The nature of the dynamic disorder of the structure could therefore be directly associated with the inherent geometric flexibility of the system. Following this formalism, in our simulations, $s = s_0$ corresponds to 1000 K with λ equal to that for real silicates (245 Nm^{-1}). Most of the simulation runs were performed at s_0 but results were also obtained at $s = 2s_0$ and $10s_0$ (superstiff).

2.2 Quartz

Calculations performed on the quartz structure, using the same model as outlined, have extended the study considerably. Quartz has a significantly different RUM spectrum to cristobalite. In the high temperature β-phase, quartz has RUMs lying along several lines and one plane in **k**-space (Giddy et al. 1993; Hammonds et al. 1996) in contrast to the several planes of cristobalite. In each simulation, the quartz sample was initiated in one of the two low-temperature α-phase configurations, with geometrically perfect tetrahedra, an Si—O distance of 1.61 Å and the unit cell volume corresponding to that found experimentally at T_c. This volume is approximately midway between the 0 K α-phase volume (Smirnov and Mirgorodsky 1997) and the *ideal* (in the same sense as used for cristobalite) β-phase volume. Therefore, just as in the case of cristobalite, the quartz tetrahedra find themselves in a box too small to allow full rotations to give the ideal atomic positions of the β-phase, and slight tetrahedral tilts may prove favourable. On stiffening the tetrahedra by the method described in the previous section, the effect that the lower degree of geometric flexibility has on the freedom of the tetrahedral rotations is explored by evaluating probability density functions for the oxygen positions at the vertices of the tetrahedra. The tendency of a framework structure to disorder dynamically purely as a consequence of the number of RUMs available for it do so is thus examined.

Calculations were performed at the same tetrahedral stiffnesses as for cristobalite to allow the two systems to be directly compared under similar conditions.

3 Results: fluctuations in k-space

Molecular dynamics simulations allow for several variables to be calculated at regularly spaced time steps, and **k**-space results are thus readily calculable. One such function is $S(\mathbf{k})$, defined in the previous section. It will be referred to here as the scattering factor. The function $S(\mathbf{k})$ is proportional to the thermal diffuse scattering intensity measured in experiments. Of course, the two quantities are not exactly the same since experimental effects such as multi-phonon scattering and atomic scattering factors have not been taken into account, but the calculation should give a good indication of the true scattering distribution.

▶

Fig. 2a–c Shaded contour plots illustrating the $S(\mathbf{k})$ intensities of β-cristobalite at a tetrahedral stiffness of s_0 viewed down the **a** [001], **b** [111] and **c** [1$\bar{1}$0] directions. These plots represent results from the simulations which are equivalent to the diffuse scattering TEM images of Withers et al. (1989)

The first illustrations of the scattering factor are views of $S(\mathbf{k})$ in planes. For each view of the function (Fig. 2a–c) a shaded contour plot is shown and the directions of diffuse intensity may be directly compared with the TEM images found of Welberry et al. (1989), Withers et al. (1989) and Hua et al. (1988), which was attributed to concerted tetrahedral motions. When comparing the MDS images viewed down various axes with those obtained by TEM, strong diffuse scattering occurs along the same directions in **k**-space in both experiment and calculation. This is evidence that the model system behaves very similarly to the true material. In fact, the regions of high intensity on the $S(\mathbf{k})$ plots of Fig. 2a–c occur at the same points as RUMs have been shown to occur for the ideal β-cristobalite structure (Hammonds et al. 1996), namely on the $\langle 110\rangle$ zones in reciprocal space. Therefore the description of the *real* structure in terms of the *ideal* modes is valid.

Of great significance is also the fact that the entire spectrum of RUMs appears to be excited, there are no regions in the $S(\mathbf{k})$ plots which would be expected to show the high intensities associated with RUMs but do not. All the RUMs are excited simultaneously and the question posed by Liu et al. (1993b) of whether RUMs may superpose without the selection of some in preference to others is thus settled: *they can*!

If the structure consisted of ordered patches of the types described by Wright and Leadbetter (1975) or Hatch and Ghose (1991) peaks would be observed on an $S(\mathbf{k})$ plot at the **k** points where the relevant phonon modes of these theories condense. The plots of Fig. 3 show $S(\mathbf{k})$ in the $\langle 1\bar{1}0\rangle$ RUM zones. No peaks are observed at the X point (001) required for the Hatch and Ghose hypothesis. The Wright and Leadbetter theory involves the RUMs at the Γ point (000) and no peak is seen here, though the magnitude of $S(\mathbf{k})$ is artificially reduced at this point due to the constraint that the system should have zero overall momentum. Around the Γ point, peaks are seen. In order to analyse the nature of these peaks, the eigenvectors of the $S_{ij}(\mathbf{k})$ matrix (Eq. 2) were found at the peaked **k** points. These eigenvectors were approximations to the normal modes of oscillation and were decomposed into their constituent parts by projecting them onto the ideal structure eigenvectors at Γ, given by the CRUSH program (Hammonds et al. 1994). It was found that an overwhelmingly large contribution to the $S(\mathbf{k})$ peaks originated from the acoustic modes (non-RUMs) which are very low in frequency near

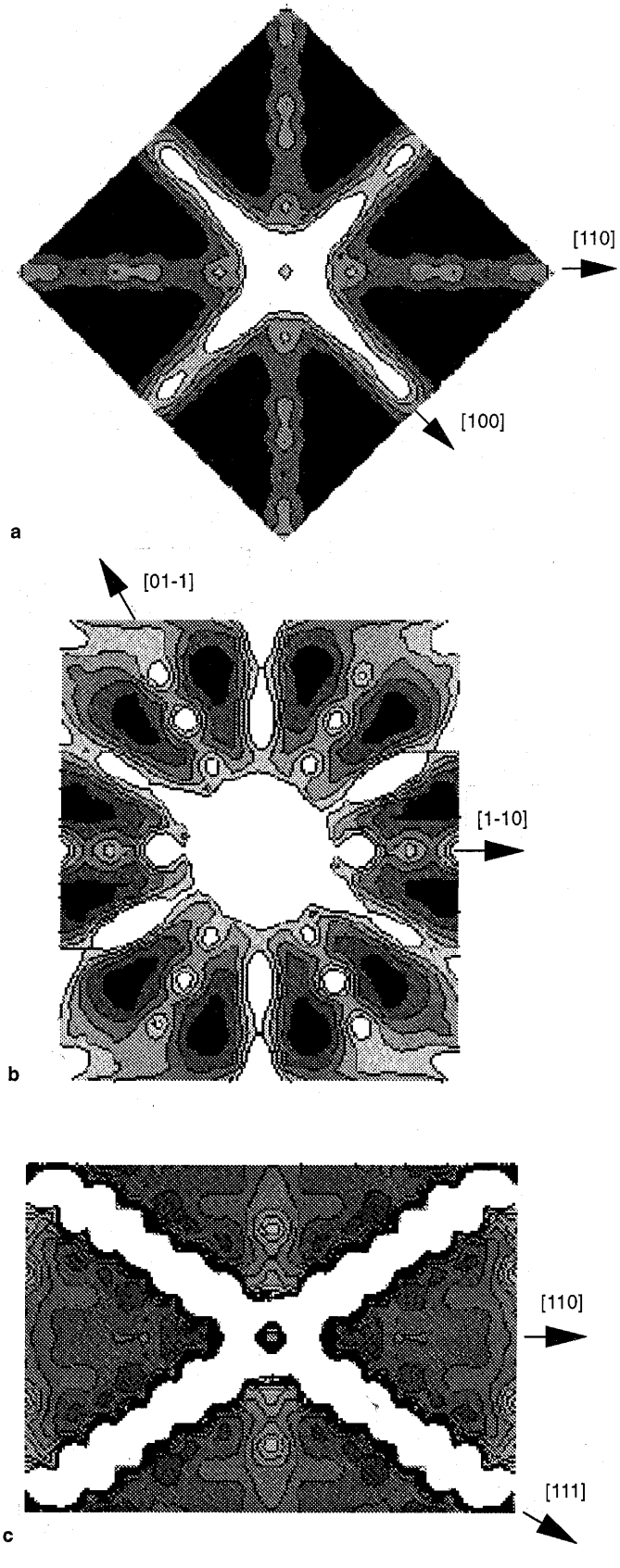

The plots of Fig. 3 show that $S(\mathbf{k})$ becomes particularly large along the [111] direction as the stiffness, s, increases. Since the entire [111] line increases in $S(\mathbf{k})$ so greatly between $2s_0$ and $10s_0$ the implication is that 'pancake' shaped domains of correlation of approximately one layer thick are forming in planes in real space perpendicular to [111]. These pancakes should have a large radius because, at a stiffness of $10s_0$, the line of peaks along [111] in $\mathbf{k}$ space has become as narrow as our resolution will allow (Fig. 4).

The structure *and the amplitude* of $S(\mathbf{k})$ on the RUM planes is changed very little in runs with superstiff tetrahedra ($s = 10s_0$). This is illustrated well by viewing the plots of $S(\mathbf{k})$ along the [001] line in Fig. 5. The plot ignores the peaked region close to the Γ point, which has been attributed to acoustic modes, and the lack of change of $S(\mathbf{k})$ with changing stiffness along these RUM lines is evident. The fluctuating disorder of the system caused by the need for the tetrahedra to tilt in concert is therefore unaffected by the tetrahedral stiffness and is inherent in the flexibility of the system.

It is possible to analyse the values of $S(\mathbf{k})$ at important points and lines in $\mathbf{k}$ space in more detail using the entries in Table 1. The ΓM ([110]) direction represents a general RUM line lying on a RUM plane and its $S(\mathbf{k})$ value is roughly half that for the ΓX ([100]) direction where two RUM planes intersect. This is as expected. Three RUM planes cross along the ΓL ([111]) direction and there is an observed increase in $S(\mathbf{k})$ here in line with that expected for the three RUMs present.

Further insights into the behaviour of the system were gained by comparing other results from simulations at different stiffnesses and temperatures. It was found that a typical non-RUM point, $\frac{3}{4}\frac{1}{4}0$, showed an $S(\mathbf{k})$ dependence on temperature which might have been predicted by Eq. (4). The drop in $S(\mathbf{k})$ is linear with temperature (Fig. 6) but there does appear to be a residual value when the extrapolated best fit line is taken to 0 K. The origin of this residual scattering lies in the inherent disordered nature of the system but its magnitude is considerably lower than that seen along RUM directions. The values of $S(\mathbf{k})$ on general points lying on RUM planes (except along the [111] direction) have been shown to remain roughly constant with increasing stiffness. The origin of these scattering values, therefore, lies in the disorder of the system.

$S(\mathbf{k})$ along the [111] direction remains roughly constant for $s = s_0$ and $2s_0$ in accordance with our interpretation but rises sharply at $10s_0$ (Fig. 3c). In order to ascertain precisely what this set of peaks in $S(\mathbf{k})$ means in terms of the structural changes at $10s_0$, it is necessary to look at real space data and this is done in the next section.

4 Real space results: correlation functions

to Γ. Therefore, there is no sign of the RUM softening required for the Wright and Leadbetter (1975) theory.

The large $S(\mathbf{k})$ values along the [111] direction imply that correlations exist in real space in planes to which

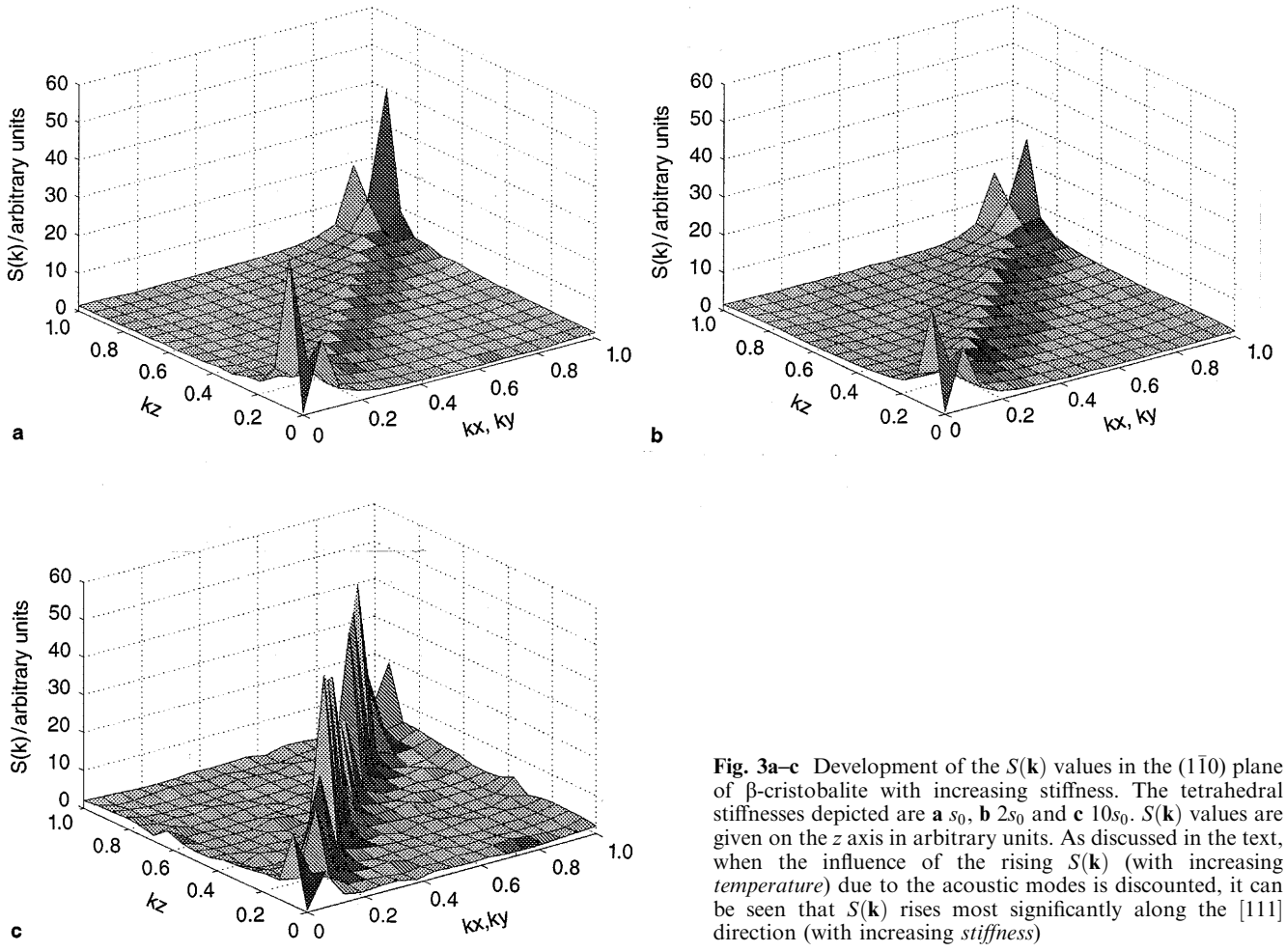

Fig. 3a–c Development of the $S(\mathbf{k})$ values in the $(1\bar{1}0)$ plane of β-cristobalite with increasing stiffness. The tetrahedral stiffnesses depicted are **a** s_0, **b** $2s_0$ and **c** $10s_0$. $S(\mathbf{k})$ values are given on the z axis in arbitrary units. As discussed in the text, when the influence of the rising $S(\mathbf{k})$ (with increasing *temperature*) due to the acoustic modes is discounted, it can be seen that $S(\mathbf{k})$ rises most significantly along the [111] direction (with increasing *stiffness*)

this direction is normal. Spatial correlation functions were therefore calculated for one of these planes by correlating the component of rotation about the [111] axis of one tetrahedron [$\phi(0)$ of Eq. (5)] with the equivalent rotations for tetrahedra at each displacement on the lattice from the first [$\phi(\mathbf{r})$ of Eq. (5)].

The plots (Fig. 7a, b) give the absolute values of the correlation function at each tetrahedral site and they

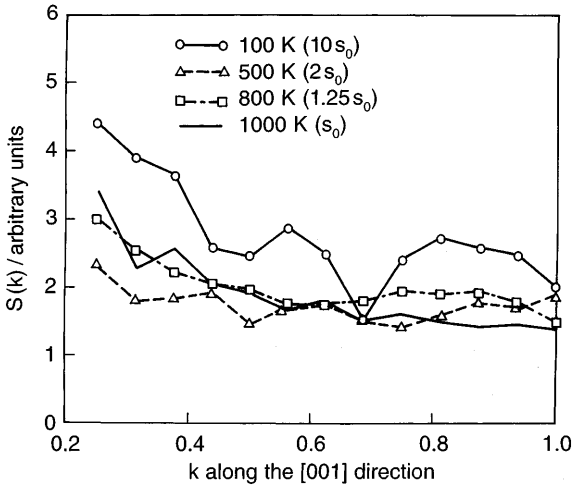

Fig. 4 $S(\mathbf{k})$ of β-cristobalite along a line on the RUM plane $(1\bar{1}0)$. The central peak occurs at the intersection with the [111] direction

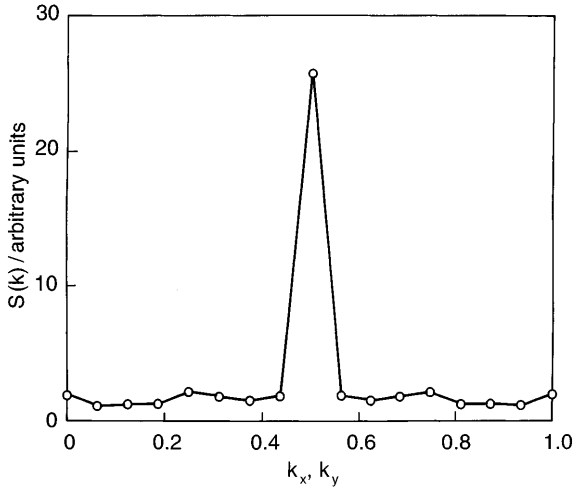

Fig. 5 $S(\mathbf{k})$ along the [001] direction in **k** space. The region close to Γ, which is influenced greatly by the acoustic modes, is excluded

Table 1 Values of $S(\mathbf{k})$ at several points and lines calculated in the simulations at a stiffness of s_0 (1000 K). The number of RUMs at each point in the ideal high cristobalite structure, as given by CRUSH, are also provided

Line/position in **k**-space	Value of $S(\mathbf{k})$ at this/these **k** point(s) (arbitrary units)	Number of RUMs at the point/along the line
ΓL [111]	4.0	3
ΓX [100]	2.9	2
ΓM [110]	1.5	1
X	1.4	2

Note: values obtained for $S(\mathbf{k})$ along lines are averaged excluding the effect of the acoustic modes close to the Γ point

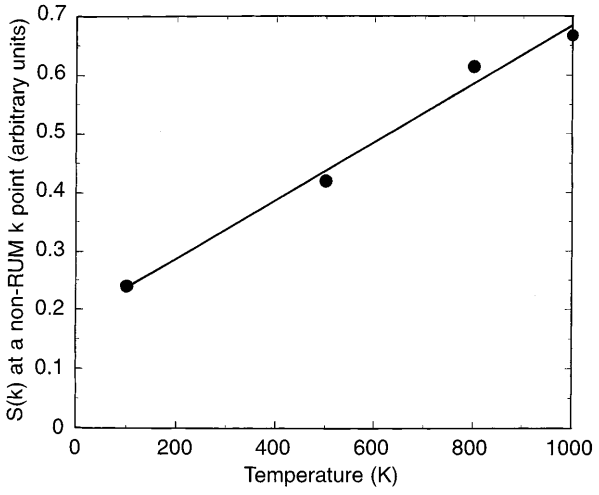

Fig. 6 Behaviour of the $S(\mathbf{k})$ function of β-cristobalite at the non-RUM point, $\frac{3}{4}\frac{1}{4}0$. $S(\mathbf{k})$ linearly decreases with temperature and the extrapolation of the best fit line shows that there is a residual value at 0 K due to the structural disorder of the system

show that, for stiffnesses of s_0 and $2s_0$, the central peak of the function has a very short range and has reached approximately 10% of its maximum value by the second to third nearest neighbours. In directions perpendicular to RUM planes (indicated by the arrows in Fig. 7a), the correlation remains at a reasonably constant value of 5%–10% for a much greater distance or decays very slowly to the edge of the sample.

At a stiffness of $10s_0$ (Fig. 7c) the magnitude of the correlations and their distances rise slightly, the magnitudes of the correlation function remain at ~10% out to the edges of the sample (outside the range of Fig. 7) and 20% values are commonly found out to the 4th and 5th nearest neighbours. This rise is the real space manifestation of the peaks seen in **k** space at high stiffness along [111]. The narrow **k**-space peaks (Fig. 4) indicate

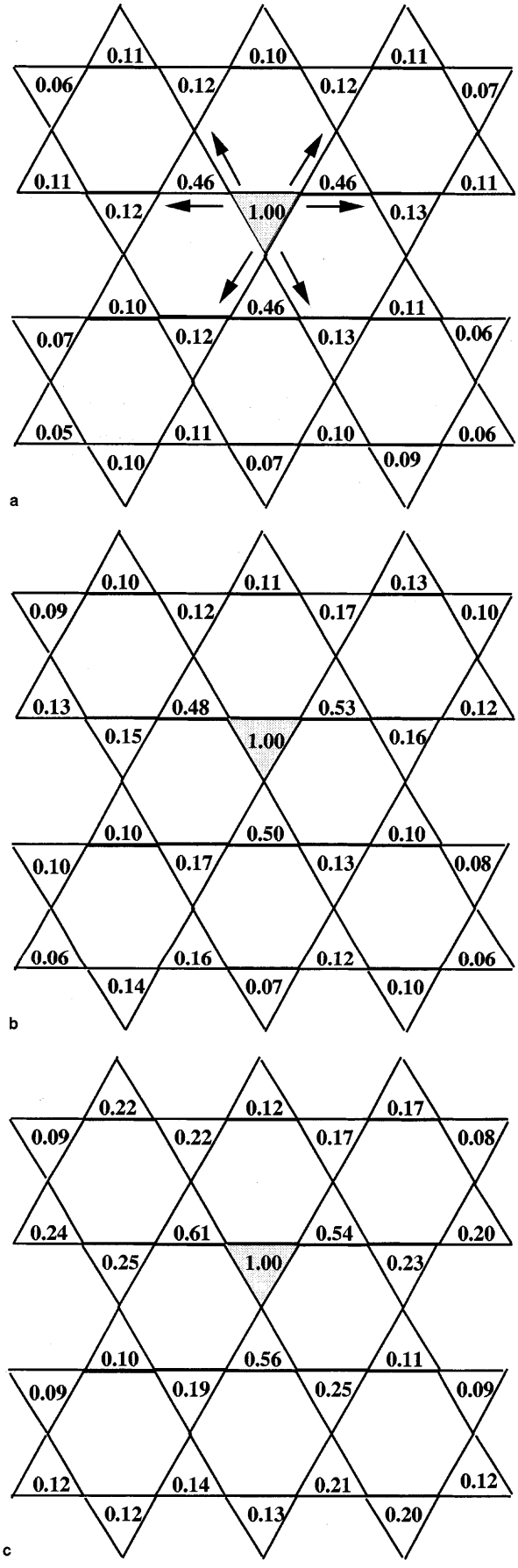

Fig. 7a–c Representations of a (111) layer of β-cristobalite. Each tetrahedron has a rotational correlation function value corresponding to the absolute value of $f_{sp}(\mathbf{r})$ in Eq. (5). **a** $s = s_0$, 1000 K, **b** $s = 2s_0$, 500 K, **c** $s = 10s_0$, 100 K

that the correlation range will be long and indeed it is but we see that this can be true without requiring the correlation value also to be large, it is $\leq 10\%$ at the sample edge.

Though there is a true increase in both the magnitude and length of the correlations for $s = 10s_0$ the central peak of the function remains very small in its range. Therefore, the sharp increase in $S(\mathbf{k})$ along the $\langle 111 \rangle$ directions in reciprocal space noted in the previous section signifies a measurable but small correlation in the planes normal to $\langle 111 \rangle$, and not a permanent, displacive change of tetrahedral orientations. The system remains essentially disordered, even at such a large stiffness. The similarity in the spatial dependences of the central peaks for all stiffnesses suggests that the structure is free to dynamically disorder as a result of its *inherent geometry* to the extent argued in Sect. 7. Due to its great freedom it does not form domains.

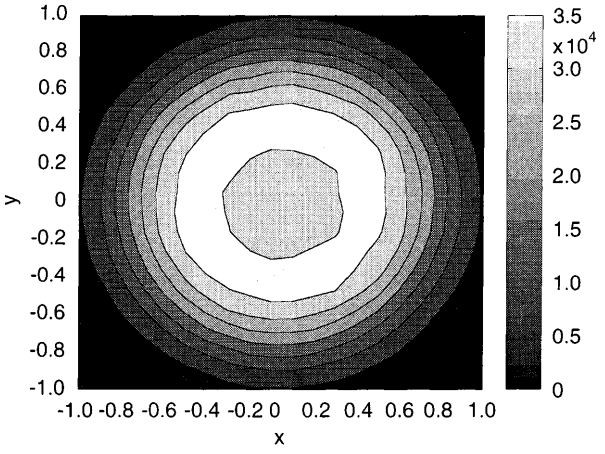

Fig. 8 A probability density plot (unnormalised) for the oxygen atoms of β-cristobalite occurring within a volume slice lying at the mid point between the average positions of neighbouring silicon atoms. The [111] (Si—Si) direction is normal to the slice and passes through its centre (0,0). The (x, y) coordinates are given in Å and the scalebar gives a relative probability scale

5 Real space results: oxygen positions

5.1 Cristobalite

In order to ascertain whether there was any localisation of the oxygen atoms at particular positions on their trajectories, probability density functions giving the probability of finding an oxygen at a certain point, were calculated. The positions of the oxygen atoms were taken to be the halfway points between the split tetrahedral vertices.

A slice of the total space surveyed, lying equidistant from the average silicon positions and containing the plane in which the annulus of oxygen positions of the static and dynamic theories should occur, is shown in Fig. 8 for $s = s_0$. The slice has a depth (into the page) of 0.05 Å and a Si—Si vector on average passes straight through the centre. The plot shows a uniform distribution of oxygen atoms about the centre with a particular concentration occurring at a radius of approximately 0.4 Å, indicating a tetrahedral tilt away from the [111] axis of $\sim 17°$ as expected. There is no sign of preferred spots of oxygen atoms at this stiffness. A similar result was obtained from Monte Carlo simulations using realistic potentials by Welberry et al. (1989), from molecular dynamics by Swainson and Dove (1995b), and from reverse Monte Carlo analysis of total neutron scattering data by Keen and Dove (to be published).

The equivalent results obtained at a stiffness of $10s_0$ are compared with those for s_0 in Fig. 9a, b. The height of the surface at each point represents the probability of finding an oxygen atom there. It can be seen that there is a greater localisation of the oxygen atoms at the annulus around the [111] direction at $10s_0$ than at s_0 and subsequently oxygens are less likely to be found passing through the [111] axis. The annulus depicted in Fig. 9b is more rugged than that of Fig. 9a suggesting that some spots may correspond to lower system energies than others. However, the extent to which the oxygen atoms

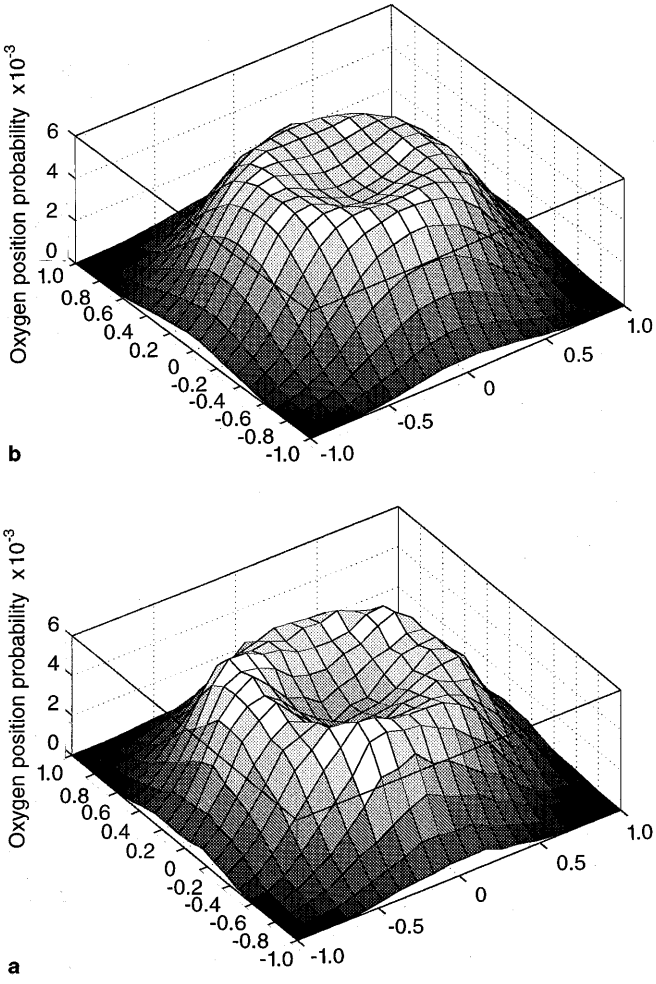

Fig. 9a, b The probability of finding an oxygen at each point within the volume slice described in Fig. 8. **a** Shows results for $s = s_0$ and **b** for $10s_0$

are found on some spots upon the annulus rather than others is almost negligible.

5.2 Quartz

The positions of the oxygen atoms in the structure of quartz do not lend themselves to be plotted in so simple a manner as is possible with cristobalite, where they fall upon easily visualisable planes. Therefore, given that the oxygen atoms in α-quartz lie on the 6(c) positions of the $P3_221$ space group, it was possible to use their general fractional coordinates, in terms of the variables x, y and z (as defined in the International Tables of Crystallography) to form order parameters for the $\alpha_{\pm}$ phases. Certain linear combinations of the x, y and z variables result in characteristic values for the $\alpha_{\pm}$ phases and are zero in the β-phase (Tautz et al. 1991). Two such order parameters are $(1/6 - z)$ and $(x - 2y + 1)$ for the left-handed enantiomorph of quartz simulated here. These were calculated in our simulations since they allowed us to locate the oxygen atoms in the x-y plane and the z direction which resulted in the two dimensional plots of Fig. 10a–c. These clearly display the degree to which the oxygen atoms are localised at three stiffnesses. In marked difference to the results of β-cristobalite, in β-quartz the oxygen atoms tend to localise at particular sites as the stiffness is increased in the high phase. Since the system is initiated in the α_+ phase, it is these sites which are occupied at very high stiffness, $10s_0$. It should be stressed that the system is vibrating at the β-quartz volume so such a localisation is not a trivial point. The qualitative difference between the two structures is clear, the significantly lower number of RUMs in β-quartz denies the structure the necessary freedom to flex like a bicycle chain and instead, at very high tetrahedral stiffness, it is 'locked' into a lower symmetry static state.

6 Time correlation functions

In addition to the real space correlation functions displayed, it is necessary in any discussion of short range order to address the issue of the lifetimes of any ordered regions. For the purposes of this study it is deemed that decay times greater than the phonon period of the lowest frequency mode of oscillation of the system are significant. These approximate RUMs have frequencies in the region of 1 THz which also compares well with experimental measurements of the low frequency modes (Swainson and Dove 1993a).

The time-dependent functions were computed as generally as possible, as detailed in the 'molecular dynamics model' section (Eq. 6).

For all domain formations, rotations of the tetrahedra persist locally. Any correlation function containing values of the rotation angles should reveal the existence of such a persistence. Therefore, the pure rotational components of the matrix $g_{ij}(t)$ were linearly combined to form the rotational time dependent function $f_{time}(t)$ where

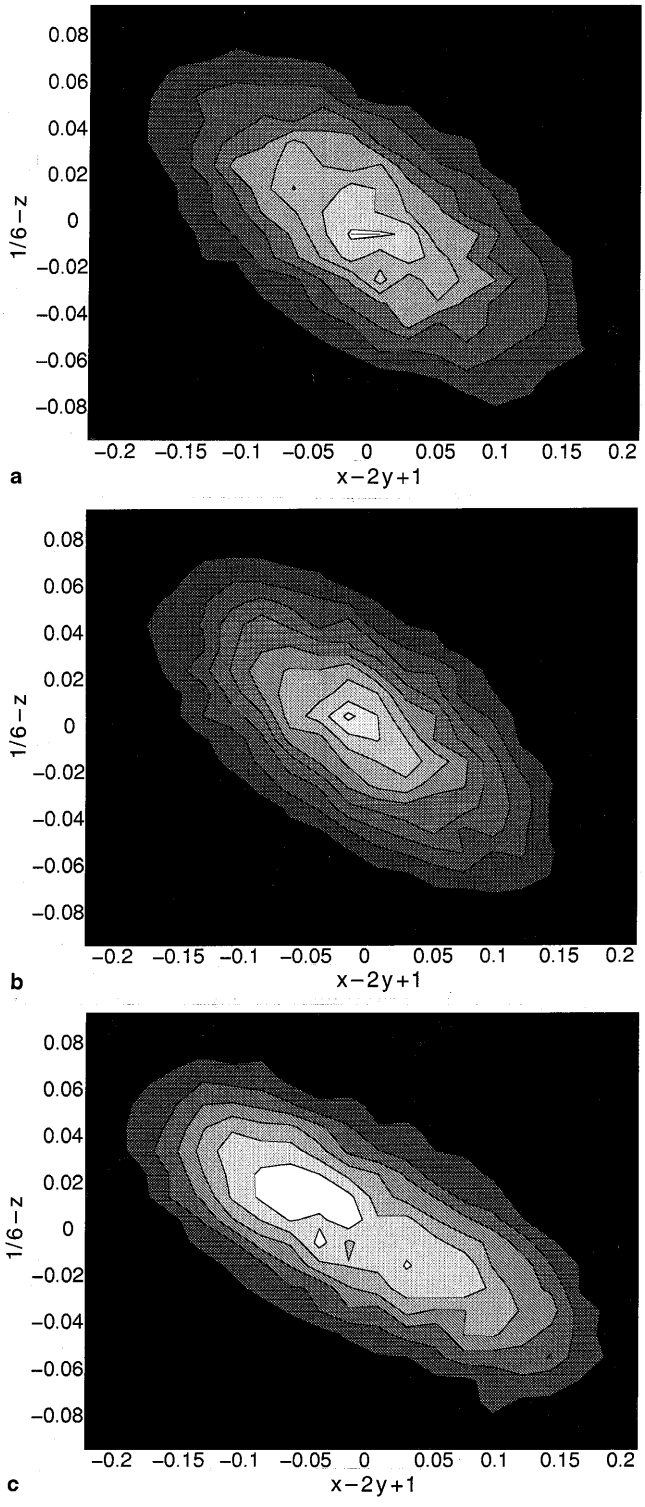

Fig. 10a–c Contour maps showing the number of oxygen atoms located within specific regions of the order parameter space for β-quartz described in the text ($(x - 2y + 1)$ and $(1/6 - z)$ being the order parameters). Three tetrahedral stiffness are represented: **a** s_0, **b** $2s_0$ and **c** $10s_0$. Order parameter coordinates of $(0.029, -0.075)$ and $(-0.029, 0.075)$ correspond to the α_+ and α_- phases of quartz at the system volume

$$f_{time}(t) = \left\langle \left(\sum_{n=1,2} \sum_{i=x,y,z} \theta_{n,i}(t) \right) \times \left(\sum_{n=1,2} \sum_{i=x,y,z} \theta_{n,i}(0) \right) \right\rangle . \quad (8)$$

The function is found by summing the rotation angles (θ) for each tetrahedron in a primitive cell ($n = 1, 2$) about the three Cartesian axes ($i = x, y, z$) and therefore this linear combination is a projection of the tetrahedral rotations about [111].

It is seen from the plot of Fig. 11 that the correlation value for β-cristobalite at s_0 has decayed to a value lower than 10% within the oscillation period of even the lowest frequency phonons of the system (~1 ps). The function contains all rotational correlations and any local static patterns involving tetrahedral rotations would have resulted in a much longer decay time than that observed.

7 Discussion and conclusions

The simulation results show that there is no static structure in the model of β-cristobalite. Given that the simulation contains much of the essential physics of the true system it is therefore inferred that β-cristobalite does not consist of a collection of short range domains, each made up locally of coupled, rotated tetrahedra. The definition of an effectively static environment, in this study, was taken to be one which did not alter significantly over the time scale of the longest phonon oscillation periods. The striking similarity of the TEM images and the scattering function calculated during simulations shows unequivocally that the entire set of RUMs is responsible for the low frequency dynamics and disorder of the crystal.

The domain theories of Hatch and Ghose (1991) and Wright and Leadbetter (1975) are ruled out by various analyses of the data. *Firstly*, there are seen to be no peaks at the **k** points of the scattering factor, $S(\mathbf{k})$, corresponding to the modes which should condense to give the local domain structures. *Secondly*, the real space correlation functions calculated have very much shorter ranges than those expected for such functions given the existence of domains. *Thirdly*, contour plots of oxygen positions reveal that there are no preferred spots lying on the annuli around the ⟨111⟩ axes as would occur for domains of the types predicted.

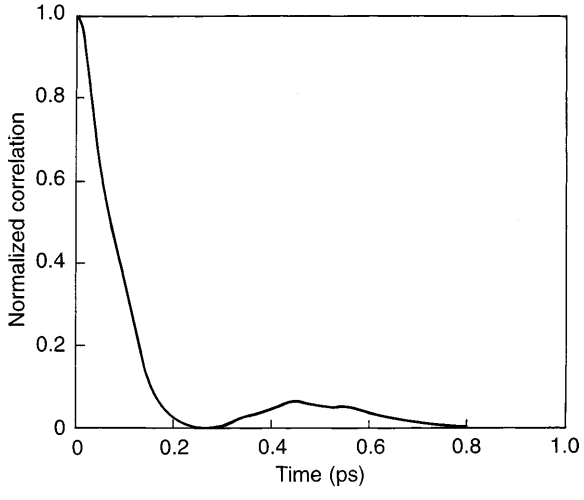

Fig. 11 The time correlation function $f_{time}(t)$ for rotations of tetrahedra in β-cristobalite about the [111] axis as detailed in the text (Eq. 8) at $s = s_0$

Stiffness increases from $s_0 \rightarrow 10s_0$ result in no changes in the $S(\mathbf{k})$ function other than the appearance of peaks along the [111] direction. The long range correlations normal to the ⟨111⟩ directions, implied by the existence of these peaks, are found to exist at $10s_0$ but had a low correlation magnitude of ≈10%. Mathematically, the Fourier Transform of the $S(\mathbf{k})$ function over **k** space, which results in the real space correlation function, gives a short range central peak (roughly out to the second nearest neighbours). The extra contribution to this integral given by the peaks along the ⟨111⟩ directions in **k** space serves to cause a long range but low amplitude correlation at a stiffness of $10s_0$ so that the structure is still disordered.

An enhanced correlation is intuitively expected with increased stiffness (or decreased temperature) since the tetrahedra become more confined to rotated orientations. As a consequence, oxygen atoms are positioned with greater probability on annuli around the ⟨111⟩ axes as demonstrated by Fig. 9. This rotational confinement results in the increased correlation values of Fig. 7c.

The lack of a significant change observed in the real space correlation function when the stiffness of the tetrahedra are increased provides a preliminary indication that the freedom of the structure is practically independent of the stiffness. The RUMs of the system are able to superpose on one another and result in local rotations to satisfy the constraint that the Si—O—Si angles lie between 140°–150°. Further to this, the contour plots of the oxygen positions show that in the β-cristobalite structure a tenfold increase in tetrahedral stiffness does not bring about a confinement of the tetrahedra to particular rotations; they rotate freely on the annuli around the ⟨111⟩ axes. Unlike β-cristobalite, the oxygen atoms in β-quartz *do* tend to localise when the stiffness is increased. This phenomenon is therefore strongly related to the number of RUMs available to the structure to permit rotations of the tetrahedra when the energy penalty paid for non-RUM motion is very high. When all but the RUM motions have been frozen out β-cristobalite remains disordered whereas β-quartz orders. The β-quartz structure has far fewer RUMs than β-cristobalite and therefore far less freedom to deform through low energy tetrahedral rotations.

An illustration of the ideas presented is given by Fig. 12. Depicted here is a snapshot of a single (111) layer of tetrahedra in the cristobalite sample at a stiffness of s_0. Oxygen atoms are placed at the positions midway on the vectors linking tetrahedral vertices. It becomes

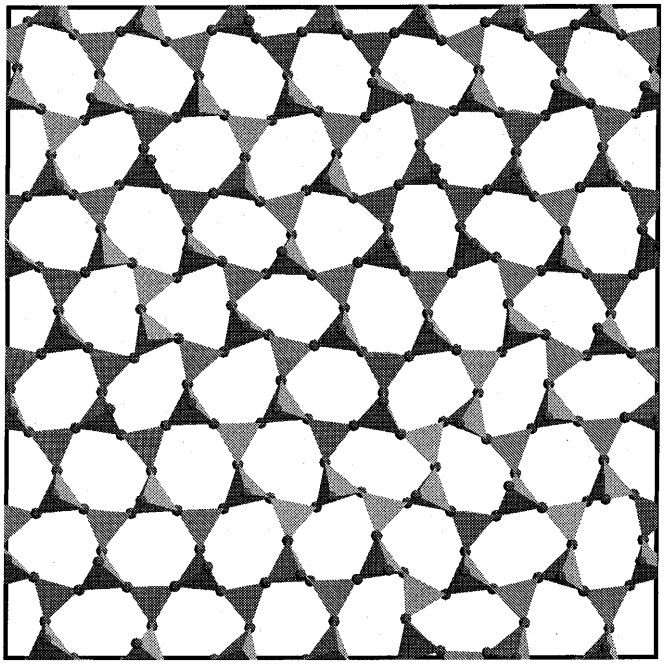

Fig. 12 A snapshot of a single (111) layer of tetrahedra in β-cristobalite viewed down a [111] direction and at a tetrahedral stiffness of s_0. The orientations of the tetrahedra may be compared with Fig. 1 and it is seen that several minimally distorting tetrahedral motions have superposed to produce a disordered configuration, six membered rings of various shapes can be seen adjacent to one another

clear how several RUMs can superpose to give an overall disordered structure. Some regions appear to show longer ranged tetrahedral rotational correlations than second nearest neighbour and this is a natural consequence of the RUM superposition model which demands a degree of short range regularity while allowing longer ranged disorder in systems with many RUMs such as β-cristobalite.

The fact that a pair of corner-sharing tetrahedra must rotate in opposite directions in order to maintain their integrity means that large amplitude RUM motions result in Si—O—Si angles between 140–150°. The $S(\mathbf{k})$ values along RUM lines such as [001] and [110] tend to remain relatively constant with changes in the kinetic temperature whereas non-RUMs $S(\mathbf{k})$s alter significantly. This observation tells us that it is the RUMs which largely contribute to the dynamic disorder of the system by effecting concerted rotations which allow oxygen atoms to occupy arbitrary positions on the annuli around ⟨111⟩ axes. Non-RUM vibrations are overlayed onto the already disordered structure which has been brought about by a superposition of all of the RUMs. This significant result states that framework crystalline systems with high degrees of *inherent geometric flexibility* may disorder easily, leading to very low correlations between stiff polyhedral units.

Acknowledgements MG would like to thank EPSRC for financial support. The computations were performed using the Hitachi SR2201 parallel computer of the Cambridge High Performance Computing Facility. We have benefited from discussion with Dr. Kenton Hammonds on both scientific and computational issues. Some of the figures were produced using 'Molecular Simulations' Cerius 2 package.

References

Bourova E, Richet P (1998) Quartz and cristobalite: high-temperature cell parameters and volumes of fusion. Geophys Res Lett 25: 2333–2336

Demkov AA, Ortega J, Sankey OF, Grubach MP (1995) Electronic-structure approach for complex silicas. Phys Rev B52: 1618–1630

Dove MT (1993) Introduction to lattice dynamics. Cambridge University Press, Cambridge

Dove MT (1997a) Theory of displacive phase transitions in minerals. Am Mineral 82: 213–244

Dove MT (1997b) Silicates and soft modes. In: Thorpe MF, Mitkova MI (eds) Amorphous insulators and semiconductors, Proc NATO AS Kluwer, Dordrecht pp 349–383

Dove MT, Giddy AP, Heine V (1993) Rigid unit mode model of displacive phase transitions in framework silicates. Trans Am Crystallogr Assoc 27: 65–74

Dove MT, Heine V, Hammonds KD (1995) Rigid unit modes in framework silicates. Mineral Mag 59: 629–639

Dove MT, Gambhir M, Hammonds KD, Heine V, Pryde AKA (1996a) Distortions of framework structures. Phase Transit 58: 121–143

Dove MT, Hammonds KD, Heine V, Withers RL, Xiao Y, Kirkpatrick RJ (1996b) Rigid Unit Modes in the high temperature phase of SiO_2 tridymite: calculations and electron diffraction. Physics and Chemisty of Minerals 23: 55–67

Dove MT, Keen DA, Hannon AC, Swainson IP (1997a) Direct measurement of the Si—O bond length and orientational disorder in the high-temperature phase of cristobalite. Physics and Chemisty of Minerals 24: 311–317

Dove MT, Harris MJ, Hannon AC, Parker JM, Swainson IP, Gambhir M (1997b) Floppy modes in crystalline and amorphous silicates. Phys Rev Lett 78: 1070–1073

Downs RT, Gibbs GV, Bartelmehs KL, Boisen MB (1992) Variations of bond lengths and volumes of silicate tetrahedra with temperature. Am Mineral 77: 751–757

Giddy AP, Dove MT, Pawley GS, Heine V (1993) The determination of rigid unit modes as potential soft modes for displacive phase transitions in framework crystal structures. Acta Crystallogr A49: 697–703

Hammonds KD, Dove MT, Giddy AP, Heine V (1994) CRUSH: a FORTRAN program for the analysis of the rigid unit mode spectrum of a framework structure. Am Mineral 79: 1207–1209

Hammonds KD, Dove MT, Giddy AP, Winkler B, Heine V (1996) Rigid unit phonon modes and structural phase transitions in framework silicates. Am Mineral 81: 1057–1079

Hammonds KD, Deng H, Heine V, Dove MT (1997) How floppy modes give rise to adsorption sites in zeolites. Phys Rev Lett 78: 3701–3704

Hammonds KD, Heine V, Dove MT (1998) Rigid unit modes and the quantitative determination of the flexibility possessed by zeolite frameworks. J Phys Chem B102: 1759–1767

Hatch DM, Ghose S (1991) The α-β phase transition in cristobalite, SiO_2. Physics and Chemistry of Minerals 17: 554–562

Hua GL, Welberry TR, Thompson JG (1988) An electron diffraction and lattice-dynamical study of the diffuse scattering in β-cristobalite, SiO_2. J Appl Crystallogr 21: 458–465

Liu F, Garofalini SH, Kingsmith RD, Vanderbilt D (1993a) First-principles studies on structural properties of β-cristobalite. Phys Rev Lett 70: 2750–2753

Liu F, Garofalini SH, Kingsmith RD, Vanderbilt D (1993b) Comment on "First-principles studies on structural properties of β-cristobalite" – Reply. Phys Rev Lett 71: 3611

Pryde AKA, Hammonds KD, Dove MT, Heine V, Gale JD, Warren MC (1996) Origin of the negative thermal expansion in ZrW_2O_8 and ZrV_2O_7. J Phys Condens Matt 8: 1–10

Pryde AKA, Dove MT, Heine MT (1998) Simulation studies of ZrW_2O_8 at high pressure. J Phys: Condens Matt 10: 8417–8428

Schmahl WW, Swainson IP, Dove MT, Graeme-Barber A (1992) Landau free energy and order parameter behaviour of the α/β phase transition in cristobalite. Z Kristallogr 201: 125–145

Smirnov MB, Mirgorodsky AP (1997) Lattice-dynamical study of the alpha-beta phase transition of quartz: soft-mode behavior and elastic anomalies. Phys Rev Lett 78: 2413–2416

Swainson IP, Dove MT (1993a) Low frequency floppy modes in β-cristobalite. Phys Rev Lett 71: 193–196

Swainson IP, Dove MT (1993b) Comment on ''First-principles studies on structural properties of β-cristobalite''. Phys Rev Lett 71: 3610

Swainson IP, Dove MT (1995a) On the thermal expansion of β-cristobalite. Physics and Chemistry of Minerals 22: 61–65

Swainson IP, Dove MT (1995b) Molecular dynamics simulation of α- and β-cristobalite. J Phys: Condens Matt 7: 1771–1788

Tautz FS, Heine V, Dove MT, Chen X (1991) Rigid unit modes in the molecular dynamics simulation of quartz and the incommensurate phase transition. Physics and Chemistry of Minerals 18: 326–336

Trachenko K, Dove MT, Hammonds KD, Harris MJ, Heine V (1998) Low-energy dynamics and tetrahedral reorientations in silica glass. Phys Rev Lett 81: 3431–3434

Welberry TR, Hua GL, Withers RL (1989) An optical transform and Monte Carlo study of the disorder in β-cristobalite. J Appl Crystallogr 22: 87–95

Welche PRL, Heine V, Dove MT (1999) Negative thermal expansion in Beta-Quartz. Physics and Chemistry of Minerals 26: 63–77

Withers RL, Thompson JG, Welberry TR (1989) The structure and microstructure of α-cristobalite and its relationship to β-cristobalite. Physics and Chemistry of Minerals 16: 517–523

Wright AF, Leadbetter AJ (1975) The structures of the β-cristobalite phases of SiO_2 and $AlPO_4$. Philos Mag 31: 1391–1401